

# Comparative experimental and numerical study of the impinging flow field of a sweeping jet

C. D'Angelo<sup>1\*</sup>, C. S. Greco<sup>1</sup>, G. Paolillo<sup>1</sup>, G. Cardone<sup>1</sup>, T. Astarita<sup>1</sup>

<sup>1</sup> University of Naples “Federico II”, Department of Industrial Engineering, Naples, Italy

\* cristina.dangelo@unina.it

Sweeping jet fluidic oscillators are devices able to convert a steady jet into an oscillating jet due to intrinsic flow instability mechanisms; the oscillations are entirely self-induced and self-sustained (Bobusch et al. (2013)). Because of their simplicity, reliability, and low maintenance costs, the interest in fluidic oscillators has remarkably grown over the last years; indeed, recent research on separation control, noise reduction, combustion control and film cooling employs air and other gases as a working fluid.

In the current work the external flow fields of three sweeping jet devices analysed through the application of the planar PIV technique are compared with the results obtained through numerical simulations.

A sketch of the experimental apparatus and the representation of the numerical computational domain are shown in Figure 1.

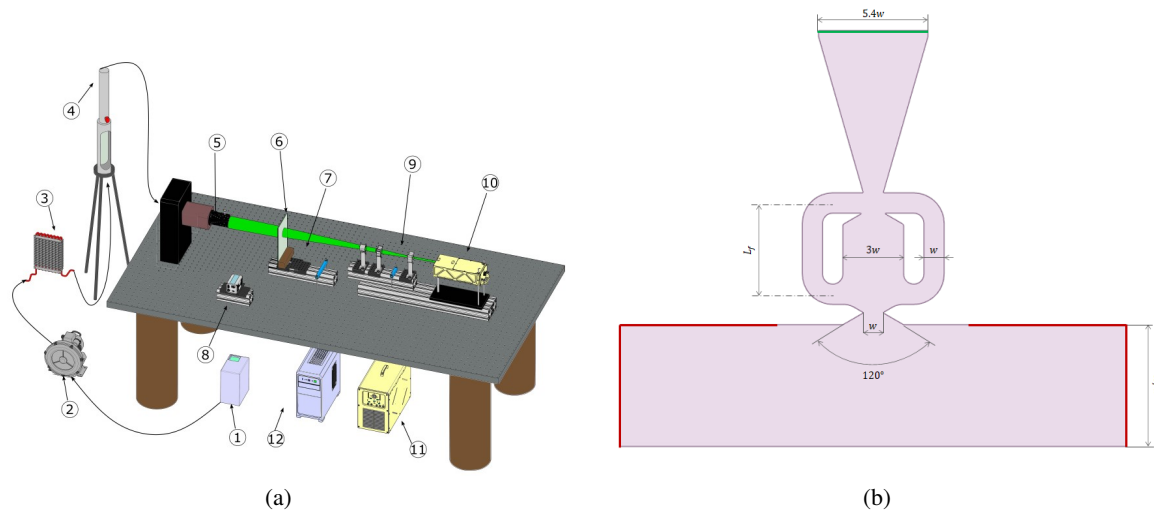


Figure 1: (a) Schematic representation of the experimental setup: inverter (1), blower (2), heat exchanger (3), flow meter (4), nozzle (5), impinging plate (6), traversing system (7), camera (8), optical lens (9), laser (10), laser power supply (11), computer (12); (b) numerical computational domain.

Three sweeping jet devices, characterized by different mixing chamber lengths ( $L_f/w = 2.5, 3.5, 4.5$ , being  $w = 0.01\text{m}$  the width of the throat section of the fluidic oscillator), are investigated and their impinging flow fields are evaluated for non-dimensional nozzle-to-plate distances  $H/w$  ranging between 2 and 6, in both the experimental and numerical analyses. All the analyses are performed at the same value of the Reynolds number ( $1.7 \times 10^4$ ). In the employed experimental apparatus the impinging plate is mounted on a translation stage in order to allow the variation of the nozzle-to-plate spacing  $H/w$ . The flow is seeded with olive oil particles generated by a Laskin nozzle. The region between the nozzle and the impinged plate is illuminated by a laser sheet 1 mm thick, provided by a Quantel Evergreen laser. The laser sheet passes through the transparent impinging wall and illuminates the entire domain, following the streamwise direction of the flow.

The numerical analyses are performed through the use of the software *Ansys Fluent*. The 2D computational domain, shown in Figure 1(b), is considered; a velocity inlet condition is set on the green segment,

with a velocity magnitude equal to 4.81 m/s, and a pressure outlet condition is set on the red segments, with a gauge pressure equal to 101325 Pa (Figure 1(b)). On the other segments of the computational domain a wall condition is imposed. The meshes of the devices are generated using *Ansys Meshing tool*; triangular elements are employed. In order to increase the accuracy of the solution in proximity of the wall, a mesh inflation is generated on each wall in order to have a  $y^+ = 1$ . A second order Semi-Implicit Method for Pressure Linked Equations (SIMPLE) is adopted to solve the 2D Unsteady Reynolds Averaged Navier-Stokes equations. A first order Shear Stress Turbulence (SST)  $k - \omega$  model is chosen in the present study for its reliability in turbulence prediction (Menter (1994)).

Both the experimental and the numerical analyses show that by increasing the distance from the plate the jet no longer sweeps in a rigid-like way from one side to the other.

As regards the influence of the mixing chamber length, in agreement with the numerical work of Seo et al. (2018), it has been found that for the devices having  $L_f/w < 4.5$  no sweeping oscillation of the jet can be detected, indeed, the twin-jet structure turns into a classical single-jet structure in these configurations. This phenomenon is evident in the contour maps of the time-averaged axial velocity field for the three devices investigated (Figure 2). All the values of the axial velocity in the contour maps are divided by a reference velocity  $U_0 = 26$  m/s.

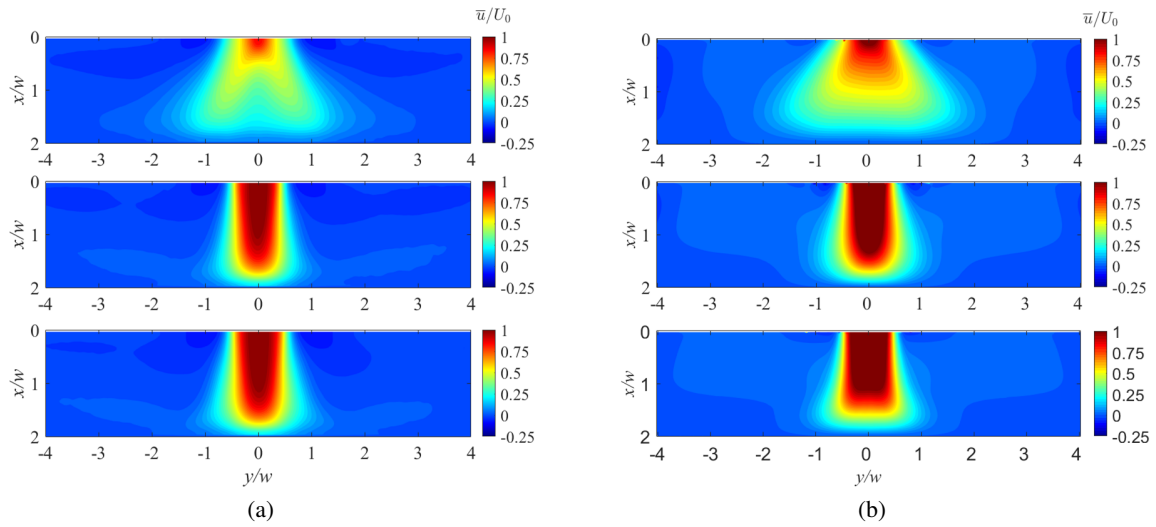


Figure 2: Experimental 2(a) and numerical 2(b) distribution of the time-averaged velocity for the three investigated devices (from top to bottom,  $L_f/w = 4.5$ ,  $L_f/w = 3.5$ ,  $L_f/w = 2.5$ ), at  $H/w = 2$ .

Furthermore, the oscillation frequency of the sweeping jet has been computed from the spectrogram of the signal of the pressure drop between the inlet and outlet section of one feedback channel. Experimentally, for the device having  $L_f/w = 4.5$  it has been found that the oscillation frequency is equal to 50 Hz; from the numerical analysis, instead, an oscillation frequency equal to 37 Hz has been computed. This difference may be due to three-dimensional effects of the experimental fluidic device, which are not captured by the 2D numerical simulations.

## References

- Bobusch BC, Wozidlo R, Bergada J, Nayeri CN, and Paschereit CO (2013) Experimental study of the internal flow structures inside a fluidic oscillator. *Experiments in fluids* 54:1–12
- Menter FR (1994) Two-equation eddy-viscosity turbulence models for engineering applications. *AIAA journal* 32:1598–1605
- Seo J, Zhu C, and Mittal R (2018) Flow physics and frequency scaling of sweeping jet fluidic oscillators. *AIAA Journal* 56:2208–2219